Regular Article

PHYSICAL CHEMISTRY RESEARCH
Published by the
Iranian Chemical Society
www.physchemres.org
info@physchemres.org

Phys. Chem. Res., Vol. 9, No. 4, 623-636, December 2021
DOI: 10.22036/PCR.2021.279882.1904

The Electronic Response of Pristine, Si, and Al-doped $B_{12}N_{12}$ Nanocage to an Ecstasy Drug: A DFT Study

E.S. Fatemi[a,b] and M. Solimannejad[a,*]

[a]*Department of Chemistry, Faculty of Science, Arak University, Arak 38156-8-8349, Iran*
[b]*Institute of Nanosciences and Nanotechnology, Arak University, Arak 38156-8-8349, Iran*

(Received 2 April 2021, Accepted 10 June 2021)

In the present research, the interaction of 3,4-methylenedioxy-N-methylamphetamine (MDMA) drug with the pristine, Si, and Al-doped $B_{12}N_{12}$ nanocage, is investigated systematically using the density functional theory (DFT) method at B97D/6-31G(d) computational level. The obtained results show that MDMA drugs can be detected after interaction with pristine $B_{12}N_{12}$. Improvement in sensing properties of the desired nanocage is achieved after doping B atom of nanocage with Al or Si atoms. The uptake of the MDMA drugs prompts a substantial change in the energy gap (E_g) of the desired frameworks. The Si-$B_{12}N_{11}$ nanocage is a more proper sensor than the pristine and Al-doped $B_{12}N_{12}$ nanocage, considering significant changes in electronic properties and appropriate recovery time. The NBO analyses reveal that charge transfer occurs from the MDMA drug to the studied nanocages.

Keywords: DFT, Sensor, MDMA drug, $B_{12}N_{12}$

INTRODUCTION

Nanotechnology is used to design and build functional, physical, chemical and biological systems in life. Nanosciences offer a range of new materials and new properties that can be used for biological and chemical sensors. Nanomaterials with unique properties such as magnetic, unusual optical, catalytic and mechanical properties can be utilized to develop current sensors that can lead to modifying spatial resolution, faster response times, and higher sensitivity levels [1].

Boron nitride (BN) nanostructures such as nanotubes [2], nanocapsules [3] and fullerenes [4] as electronic devices, high heat-resistance semiconductors, and gas storage materials have been extensively investigated by experimental and theoretical researchers because of their unique properties in recent years.

Boron nitride (BN) nanocage of $B_{12}N_{12}$ as the stable structure [5] was synthesized with the bandgap energy of 5.1 eV [6]. Several studies have reported on BN fullerene-like nanostructures as convenient tools for the adsorption of contaminants from aqueous solutions. This is due to their great resistance to oxidation, high stability, wide band gap, large thermal conductivity, high hydrophobicity [7-9], proper materials for encapsulation and delivery applications [10], and as a nanocatalyst with Lewis acid, Lewis-base properties [11]. During recent years, many researches have focused on adsorption of several important molecule and drug on $B_{12}N_{12}$ such as formaldehyde [12], halomethanes [13], ammonia [14], CO [15], CO_2 [16], N_2O [17], NO, H_2, N_2, and CH_4 [18], Phosgene gas [19], NH_3, and H_2O [20], HCN, and ClCN [21], pnictogen hydrides (NH_3, PH_3, and AsH_3) [22], H_2S [11], tetryl [23], tabun [24], formaldehyde monomer and dimers [25], SO_2, and O_3 [26], pyrrole [27], alprazolam drug [28], celecoxib drug [29], amphetamine [30], and Melphalan [10] using DFT methods. Abdolahi *et al.* reported the nature of interactions of sulfasalazine drug moiety with Au atom/dimer decorated $B_{12}N_{12}$ nanocluster [31]. Doping of the first-row transition metals

*Corresponding author. E-mail: m-solimannejad@araku.ac.ir

(Sc, Ti, V, Cr, Mn, Fe, Co, Ni, Cu, Zn) on $B_{12}N_{12}$ fullerene-like nanocluster has been investigated systematically by Abbasi *et al.* [32]. Baei has theoretically shown that the $B_{12}N_{12}$ sodalite-like cage is a potential sensor for hydrogen cyanide [33]. The effect of the functionalized Ni and Pd transition metals on the interaction of the mercapto pyridine (MCP) with the $B_{12}N_{12}$ has been survived by Rezaei-Sameti *et al.* [34]. Majedi *et al.* have presented the sensing possibility of the pristine, Al, and Ga-doped $B_{12}N_{12}$ nanostructures toward hydrazine and hydrogen peroxide and their analogs [35]. The performance of $B_{12}N_{12}$ nanocage as a sensing material for the detection of proline has been researched by Ahmadi *et al.* [36]. Jouypazadeh et al. researched adsorption and detection of sulfur mustard chemical warfare agent by the C_{24}, $C_{12}Si_{12}$, $Al_{12}N_{12}$, $Al_{12}P_{12}$, $Be_{12}O_{12}$, $B_{12}N_{12}$, and $Mg_{12}O_{12}$ nanocages [37]. Jalali *et al.* investigated boron nitride nanocage performance as an adsorbent and sensing material to remove and detect trinitroanisole [38]. The adsorption property of H_2 on the surface of $B_{12}N_{12}$ and Ni-decorated $B_{12}N_{12}$ nanoclusters has been studied by Shokuhi Rad *et al.* [39]. One of the present authors researched Sc-doped $B_{12}N_{12}$ nanocage theoretically for detecting toxic cyanogen gas [40].

The 3,4-methylenedioxy-N-methylamphetamine (MDMA) is the principal component of the ecstasy drug, consisting of other sympathomimetic amines, including amphetamine (AP) and methamphetamine. The MDMA leads to weak hallucinogenic properties, more accurately demonstrated as increased sensory awareness by acting on central nervous system stimulants [41].

Herein, the capability of the pristine, Si, and Al-doped $B_{12}N_{12}$ nanocage for adsorption and sensing of MDMA drugs is investigated from the electronic structure calculations, natural bond orbitals (NBO) [42], and frontier molecular orbital (FMO) [43] analysis for the first time.

COMPUTATIONAL METHODS

All calculations, including; geometry optimizations, electronic structure analyses, and the NBO charges, were performed by Gaussian 09 [44] code using density functional theory (DFT) at the B97D/6-31G(d) computational level. For representing the nature of the stationary points, frequency calculations have been carried out at the same optimization level. The adsorption energies (E_{ads}) for the interaction of MDMA and $B_{12}N_{12}$ nanocage has been obtained through Eq. (1),

$$E_{ads} = E_{complex} - E_{MDMA} - E_{nanocage} + E_{BSSE} \quad (1)$$

$E_{complex}$ is the total energy of the considered complexes, E_{MDMA} is the total energy of the drug, $E_{nanocage}$ is the total energy of the nanocage. The full counterpoise (CP) method [45] was used to correct the adsorption energy from the inherent basis set superposition error (BSSE). The HOMO-LUMO gap (E_g) of the intended systems is determined by using Eq. (2):

$$E_g = \varepsilon_L - \varepsilon_H \quad (2)$$

ε_L is the lowest unoccupied molecular orbital (LUMO) energy and ε_H is the highest occupied molecular orbital (HOMO) energy.

The percentage of change in HOMO-LUMO gap ($\%\Delta E_g$) due to complex formation is calculated from the Eq. (3):

$$\%\Delta E_g = \frac{E_g(complex) - E_g(nanocage)}{E_g(nanocage)} \times 100 \quad (3)$$

Where $E_{g\,(complex)}$ and $E_{g\,(nanocage)}$ are the HOMO-LUMO gap of $B_{12}N_{12}$ nanocage in the presence and absence of the MDMA drug, respectively. Gauss Sum program [46] has been used to draw density of states (DOS) plots. NBO analyses were performed to study charge transfer between the MDMA molecule and the adsorptive frameworks of the present study.

RESULTS AND DISCUSSION

Structural Analysis of Pristine $B_{12}N_{12}$ Nanocage and MDMA

As depicted in Fig. 1a, the $B_{12}N_{12}$ nanocage consists of six tetrahedral rings and eight hexagonal rings. Additionally, this nanocage has two different types of B–N bond lengths corresponding to each ring type. The computed average B–N length and N–B–N bond angle of the isolated $B_{12}N_{12}$ nanocage are 1.49 Å and 124.30°,

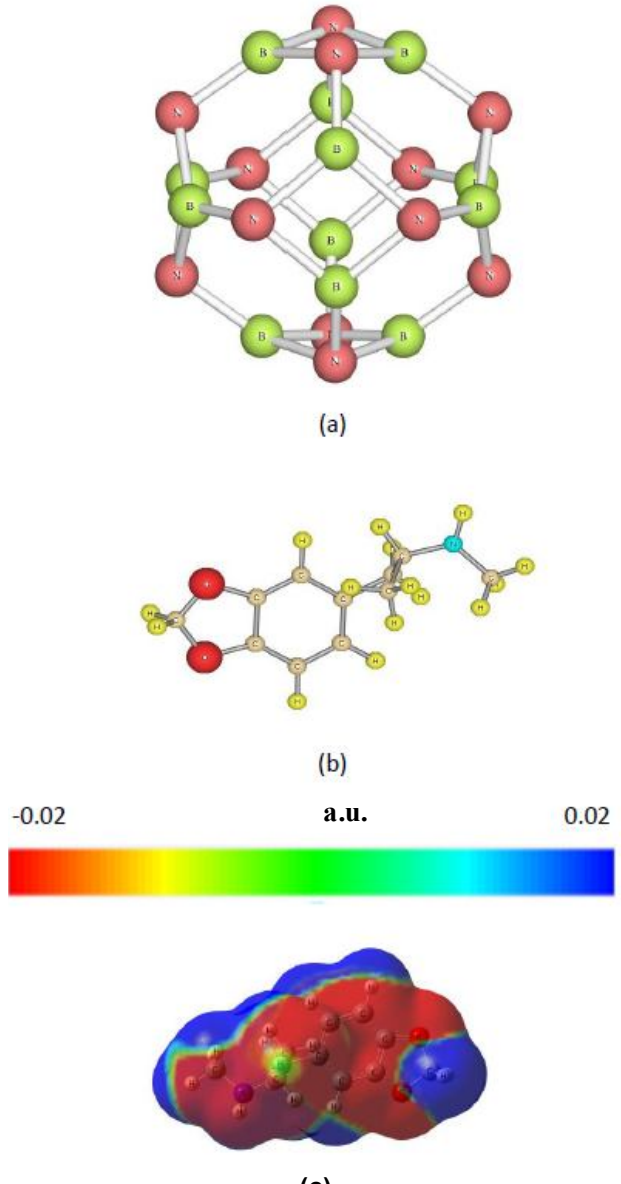

Fig. 1. (a) The optimized structure of pristine $B_{12}N_{12}$ nanocage, (b) the schematic representation of 3,4-methylenedioxy-N methylamphetamine (MDMA), and (c) MEP surface of the MDMA drug in ±0.02 a.u.

respectively. The structures of the $B_{12}N_{12}$ nanocage consist of one type of B atom. The boron atom of $B_{12}N_{12}$ nanocage operates as Lewis acid (electron acceptor), and the nitrogen atoms of nanocage serve as Lewis base (electron donor).

Table 1. The Calculated HOMO-LUMO Gap of Pristine $B_{12}N_{12}$ Based on Different Computational Methods in the Previous and Present Studies

Method	Eg (eV)	Ref.
Exp	5.1	[6]
B3LYP	6.06, 6.84	[11,15]
B97D	5.19	[15]
TPSS	5.28	[15]
B3LYP-D3	6.84	[24]
MPW1PW91	7.33	[26]
M06-2X	7.20, 9.34	[29,30]
B3PW91	6.93	[31]
PBE	4.99, 5.07	[31,33]
PW91	5.03	[33]
CAM-B3LYP	9.58	[40]
B97D	5.20	Present work

Depending on the position of atoms in the structure of the MDMA drug, it is evident that the potential places for the interaction of the drug are O1, and O2 oxygen atoms, nitrogen atom, and the center of the aromatic ring (denoted as Ar) as shown in Fig. 1b.

Moreover, the MEP plot of MDMA in Fig. 1c intelligibly show that nitrogen, oxygen atoms, and aromatic ring are convenient sites (red regions) to interact with the electrophilic moieties. The green and blue areas in Fig. 1c show the electron-deficient areas for the attraction of nucleophilic species.

Adsorption of MDMA on the Pristine $B_{12}N_{12}$ Nanocage

The calculated HOMO-LUMO gap (Eg) of pristine $B_{12}N_{12}$ at the various computational levels are listed in Table 1. According to Table 1, it is shown that the B97D method gives reliable results in good agreement with that of the experimental value of 5.1 eV [6]. So, the adsorption of MDMA on the pristine $B_{12}N_{12}$ nanocage is investigated with the B97D method. Several positions were considered for adsorption of the MDMA drug over $B_{12}N_{12}$ nanocage, as shown in Fig. 2.

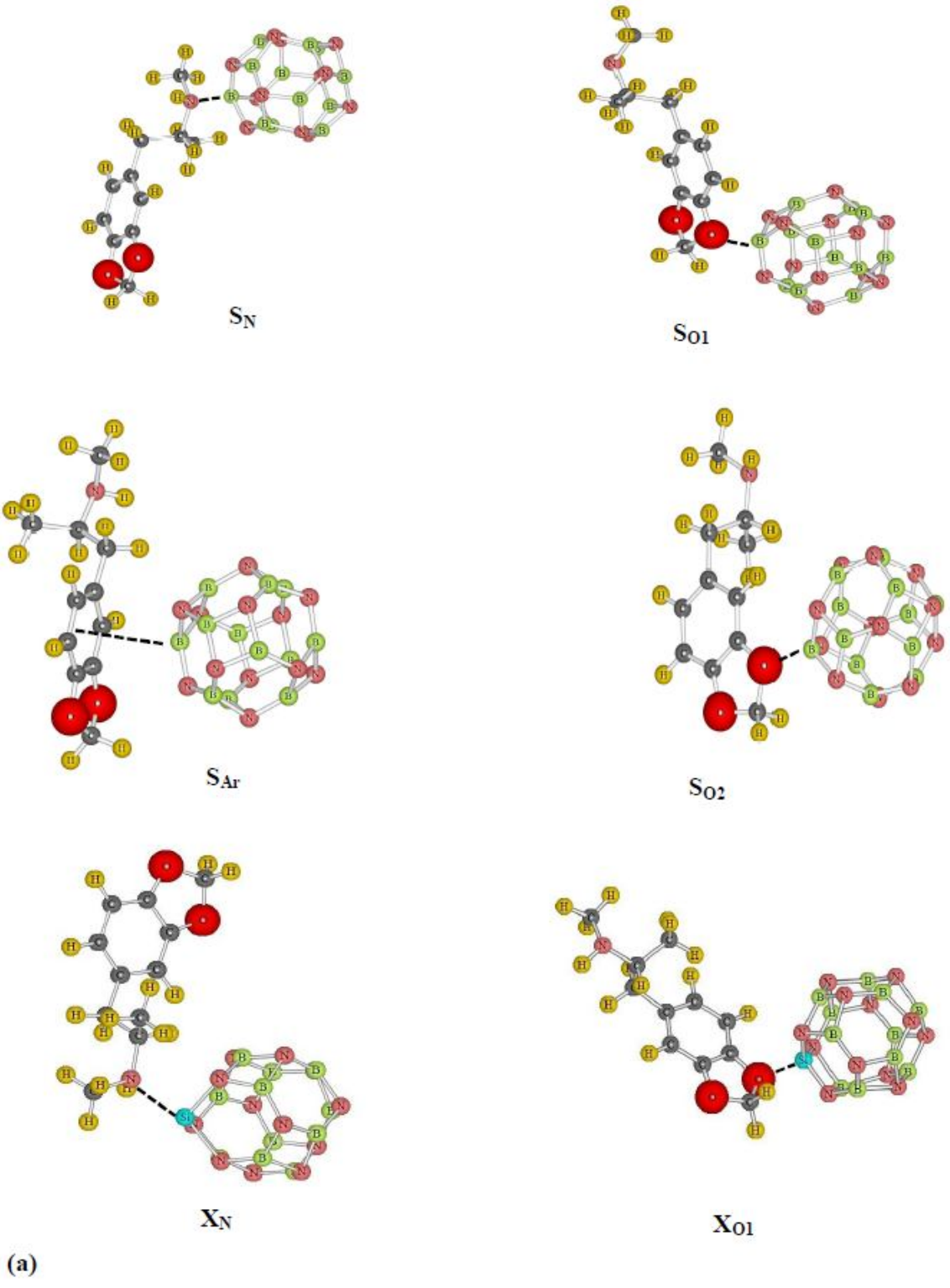

Fig. 2. Optimized structure of studied complexes at different configurations (a and b).

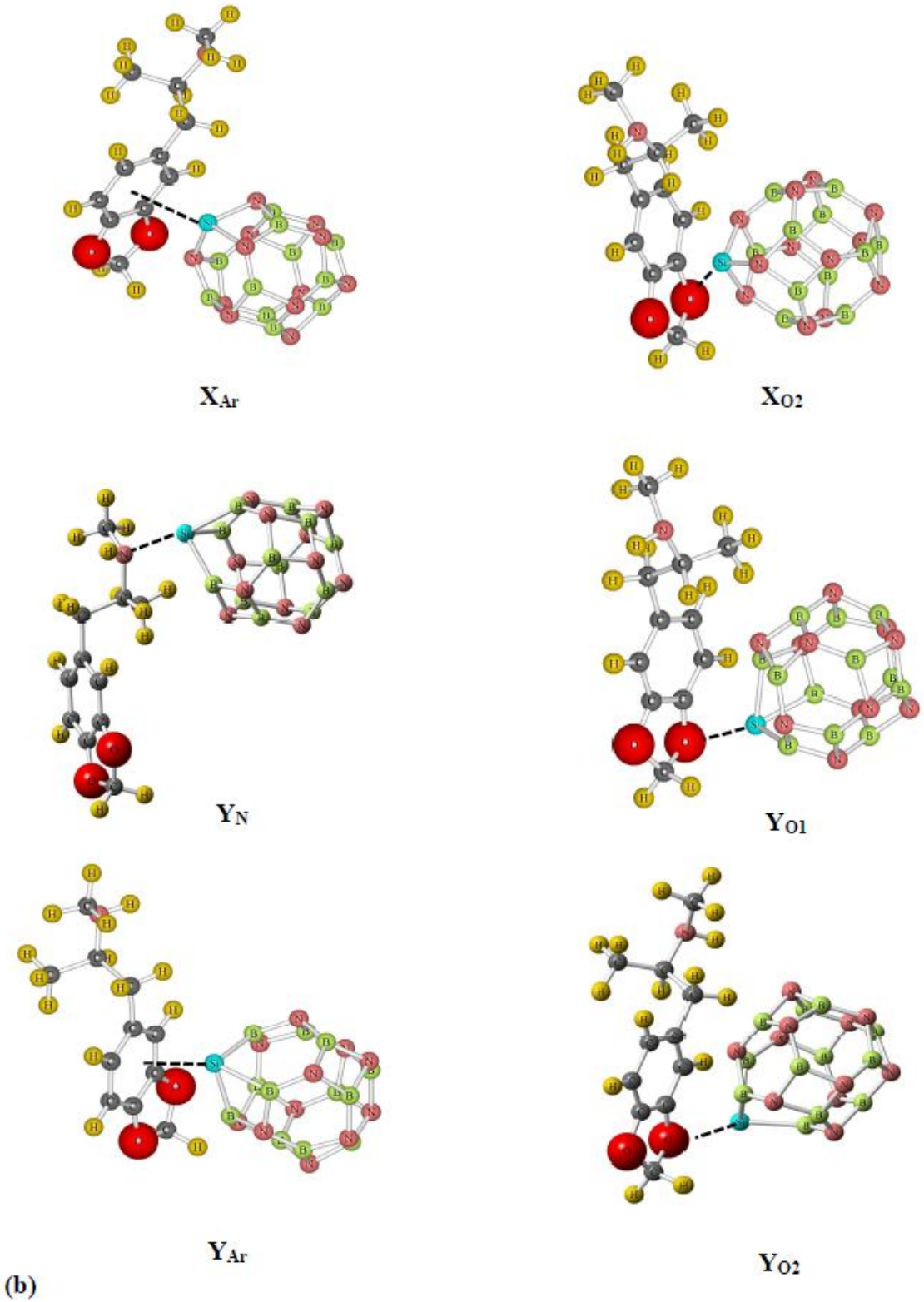

Fig. 2. Continued.

Table 2. The Calculated Adsorption Energy (E_{ads}), the Basis Set Superposition Errors (BSSE), the Lowest Vibrational Frequency (ν), HOMO, LUMO Energies, HOMO-LUMO Energy Gap (Eg), the Change of Energy Gap of Nanocage after Adsorption of MDMA Drug (%ΔEg), and Total Charge Transfer (QT) of Pristine, Si, and Al-doped $B_{12}N_{12}$ Nanocage and MDMA Complexes

Systems	E_{ads} (eV)	BSSE (eV)	ν (cm^{-1})	HOMO (eV)	LUMO (eV)	Eg (eV)	ΔEg (%)	QT (e)
$B_{12}N_{12}$	-	-	314.00	-6.71	-1.51	5.20	-	-
S_N	-1.86	0.21	13.62	-5.09	-1.16	3.93	-24.4	0.298
S_{O1}	-0.73	0.19	20.07	-4.94	-1.46	3.48	-33.27	0.245
S_{Ar}	-0.55	0.14	21.71	-4.58	-1.34	3.24	-37.70	0.092
S_{O2}	-0.75	0.20	12.88	-4.77	-1.45	3.32	-36.29	0.241
Si-$B_{11}N_{12}$	-	-	267.72	-6.55	-4.42	2.13	-	-
X_N	-1.13	0.19	16.20	-4.93	-2.99	1.94	-8.99	0.189
X_{O1}	-0.60	0.19	18.18	-4.86	-3.82	1.04	-51.10	0.219
X_{Ar}	-0.70	0.17	20.81	-4.74	-3.70	1.04	-51.46	0.129
X_{O2}	-0.69	0.19	22.27	-4.64	-3.91	0.73	-65.49	0.089
Si-$B_{12}N_{11}$	-	-	223.20	-5.85	-4.74	1.11	-	-
Y_N	-0.89	0.15	11.45	-4.73	-4.05	0.68	-38.88	0.235
Y_{O1}	-0.60	0.14	13.78	-4.79	-4.13	0.66	-41.13	0.166
Y_{Ar}	-0.68	0.14	22.60	-4.73	-4.05	0.68	-38.88	0.154
Y_{O2}	-0.60	0.13	12.96	-4.75	-4.08	0.67	-39.24	0.187
Al-$B_{11}N_{12}$	-	-	230.90	-6.32	-3.55	2.77	-	-
M_N	-2.57	0.19	14.29	-5.26	-1.34	3.92	41.35	0.213
M_{O1}	-1.66	0.18	15.88	-5.14	-1.89	3.25	17.29	0.129
M_{Ar}	-1.67	0.17	21.86	-5.28	-2.64	2.64	-4.84	0.161
M_{O2}	-1.73	0.22	18.37	-4.87	-1.85	3.02	8.72	0.123
Al-$B_{12}N_{11}$	-	-	159.31	-5.11	-3.84	1.27	-	-
N_N	-2.16	0.16	12.94	-4.13	-1.98	2.15	69.73	0.194
N_{O1}	-1.22	0.15	6.98	-4.33	-2.28	2.05	61.56	0.105
N_{Ar}	-1.29	0.16	19.11	-4.33	-2.57	1.76	39.18	0.115
N_{O2}	-1.25	0.14	10.86	-4.34	-2.28	2.06	62.44	0.147

After optimizing all the considered structures, four proper complexes for disposing the drug on the pristine $B_{12}N_{12}$ nanocage are obtained. The calculated adsorption energy (E_{ads}), the basis set superposition errors (E_{BSSE}), and the lowest frequency (ν) of optimized complexes are represented in Table 2. It is shown that the S_N is a more stable complex of adsorbed MDMA on the pristine $B_{12}N_{12}$ nanocage. In the S_N complex, the interaction between N atoms of MDMA drugs with B atom if nanocage leads to the most negative adsorption energy of -1.86 eV among the studied complexes.

The computed E_g values of the studied complexes and pristine $B_{12}N_{12}$ are listed in Table 2. The ε_H and ε_L of $B_{12}N_{12}$ were obtained at -6.71 and -1.51 eV, respectively. The formation of a high energy level as the new HOMO level locating between the original HOMO and LUMO of pristine $B_{12}N_{12}$ nanocage leads to decreased E_g values in the complexes, indicating that electronic properties of nanocage are changed due to adsorption of the MDMA drug. NBO analyses show that charge transfer occurs from MDMA

drug to the pristine $B_{12}N_{12}$ nanocage range of 0.092-0.298 e. From the results, it is clear that the magnitude of charge transfer is more for the S_N complex, consistent with more stability of this complex.

Adsorption of MDMA on the Si-doped $B_{12}N_{12}$ Nanocage

In the following, we have researched the effect of Si doping on the sensing properties of $B_{12}N_{12}$ nanocage to improve the nanosensor's efficiency in the detection of the MDMA. For this goal, two boron atoms and nitrogen atoms of $B_{12}N_{12}$ nanocage were replaced with a silicon dopant. Indeed, the adsorption of MDMA drug on the electronic properties of Si-doped $B_{12}N_{12}$ nanocages is considered. After optimization of the considered structures, eight complexes are obtained, displayed in Fig. 2. The silicon atom of Si-doped $B_{12}N_{12}$ nanocage serves as Lewis acid (electron acceptor), and the nitrogen atoms of nanocage serve as Lewis base (electron donor). The calculated adsorption energy (E_{ads}) of studied complexes, represented in Table 2. The results show that the adsorption of MDMA from nitrogen head atom on the doped Si atom of $B_{11}N_{12}$ is the most favorable interaction between MDMA and nanocage with the most negative adsorption energy -1.13 eV. The results display that E_g values of Si-doped $B_{11}N_{12}$ and $B_{12}N_{11}$ are 2.13 and 1.11 eV, respectively, as represented in Table 2. The decreasing of E_g values of Si-doped $B_{12}N_{12}$ nanocage after adsorption of the MDMA drug indicates that electronic properties of nanocage are changed substantially. The results show that for all complexes in the Si-doped $B_{12}N_{12}$ nanocage, the $\%\Delta E_{gap}$ values vary between -9 and -65%, with the most for the X_{O2} complex. Thus, the interaction of MDMA on the $SiB_{11}N_{12}$ nanocage is more prominent than the $SiB_{12}N_{11}$ nanocage. The results display that $SiB_{11}N_{12}$ nanocage may be an excellent chemical sensor to detect MDMA drug compared with the pristine $B_{12}N_{12}$ nanocage. This evidence regards that doping one of the boron atoms of nanocage with the Si atom is more favorable for interaction between MDMA drug and nanocage than replacing the N atom of nanocage with the Si atom. Overall, doping of $B_{12}N_{12}$ with the Si atom improves the sensing performance of nanocage to detect MDMA. Moreover, the results of the NBO analyses indicated the charge transfer from the drug to nanocage.

The density of states (DOS) of the X_{O2} complex with high sensing performance to detect MDMA drug is depicted in Fig. 3. Thus, the Si-doped $B_{12}N_{12}$ nanocage can be more suitable for detecting MDMA than pristine $B_{12}N_{12}$ nanocage. In the next step, the effect of doping Al atom on $B_{12}N_{12}$ nanocage is investigated.

Adsorption of MDMA on the Al-doped $B_{12}N_{12}$ Nanocage

In this research, we also investigated the effect of Al doping on the sensing properties of the $B_{12}N_{12}$ nanocage. For this purpose, the stable structures and the electronic properties after adsorption of the MDMA drug on the Al-doped $B_{12}N_{12}$ have been surveyed. This result implies that the interaction between MDMA drug and Al-doped $B_{12}N_{12}$ nanocage is strong. The most stable M_N complex is obtained from the interaction between the Al atom of $Al\text{-}B_{11}N_{12}$ nanocage with the nitrogen atom of the MDMA drug that leads to the adsorption energy of -2.57 eV. Besides, the interaction of MDMA with the Al-doped $B_{12}N_{12}$ nanocage was much stronger than the pristine and Si-doped $B_{12}N_{12}$ nanocage.

Now, let us provide a scientific explanation for the observed order for the binding strength between the drug and different nanoclusters. To justify the observed trend in the stability of the studied complexes, the magnitudes of the most positive ($V_{S,\ max}$) of the studied nanocage and most negative electrostatic potentials ($V_{S,\ min}$) on the surface of the MDMA drug have been calculated using Multiwfn code [47]. The computed $V_{S,\ min}$ for MDMA drug is -35.75 kcal mol^{-1}, and the calculated $V_{S,\ max}$ is 27.17, 29.74, 26.97, 90.74, and 62.86 kcal mol^{-1} for $B_{12}N_{12}$, Si- $B_{11}N_{12}$, Si- $B_{12}N_{11}$, Al- $B_{11}N_{12}$, and Al- $B_{12}N_{11}$, respectively. The maximum and minimum values of the $V_{S,\ max}$ correlated well with the strongest (M_N) adsorption energy and the least stable (S_N) complexes.

The results show that the most $\%\Delta E_{gap}$ value is observed for the N_N complex with 69.73%. As shown in Table 2, the sensitivity of the $Al\text{-}B_{12}N_{11}$ nanocage toward MDMA drugs is more than $Al\text{-}B_{11}N_{12}$ nanocage.

Doping of Al atom on the $B_{12}N_{12}$ nanocage plays a different role in sensing MDMA drug when compared with the effect of doping Si atom on $B_{12}N_{12}$ nanocage. Doping of the Al atom instead of the nitrogen atom of the $B_{12}N_{12}$

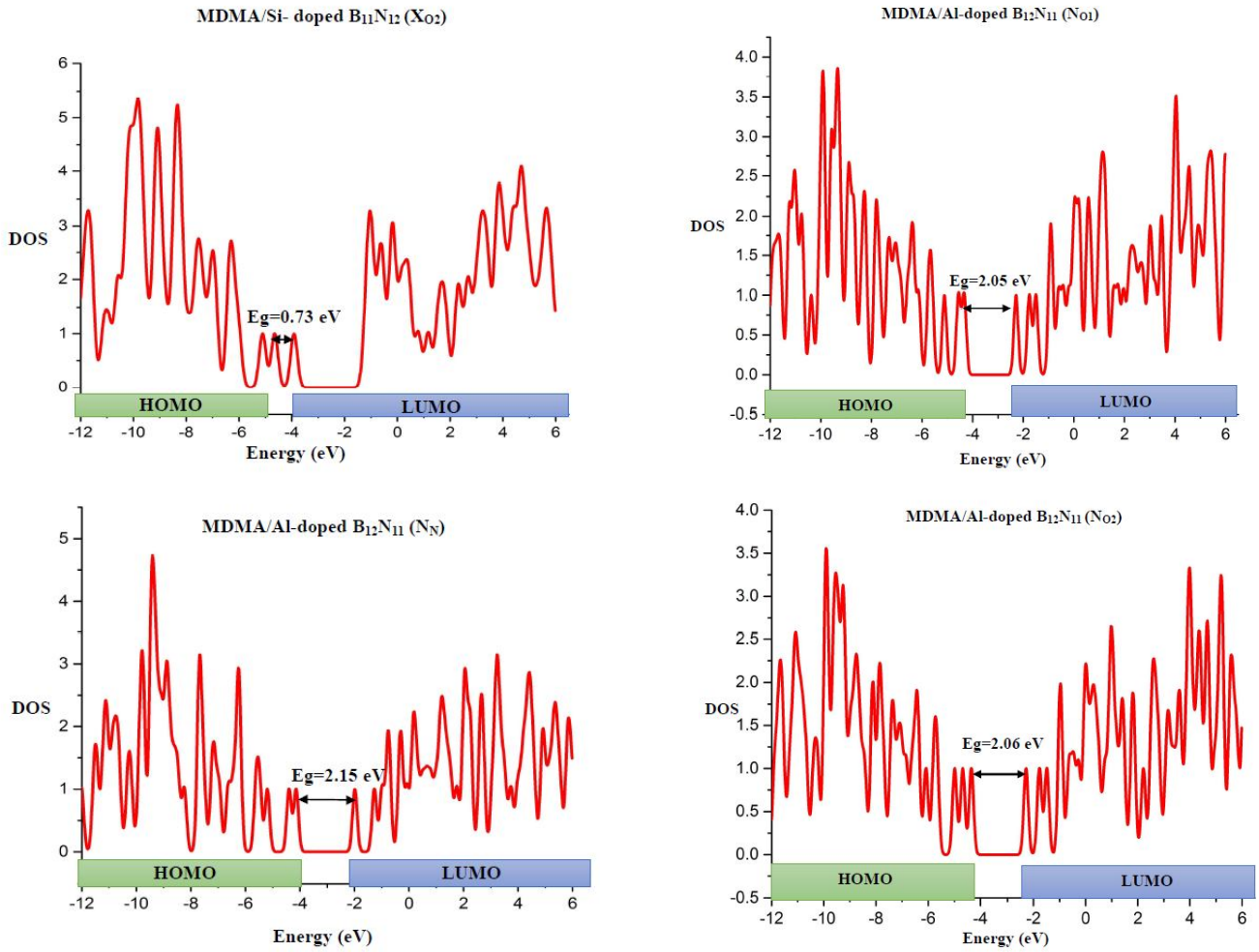

Fig. 3. The density of states (DOS) of X_{O2}, N_N, N_{O1}, and N_{O2} complexes using B97D method.

nanocage gives a more sensitive medium than pristine $B_{12}N_{12}$ nanocage. On the other, more improvement of sensing properties of the pristine $B_{12}N_{12}$ nanocage is obtained from replacing the B atom of the $B_{12}N_{12}$ nanocage with the Si atom. The obtained result also displays that the interaction of MDMA with the Al-doped $B_{12}N_{12}$ is stronger than the Si-doped $B_{12}N_{12}$ nanocage. The results show that Al-doped $B_{12}N_{12}$ may be a promising chemical sensor that plays an essential role in detecting MDMA drugs.

The density of states (DOS) of considered complexes was drawn in Fig. 3 to perceive the adsorption effect.

Based on the results of Table 2, it can be concluded that the Al-doped $B_{12}N_{12}$ nanocage is a promising sensor for detecting the MDMA drug. Besides, the sensing performance of Al-doped $B_{12}N_{12}$ toward MDMA drugs is more prominent than Si-doped $B_{12}N_{12}$.

It is necessary to check recovery time (τ) under a specific temperature to appraise the possibility of MDMA molecule desorption. Recovery time (τ) can be obtained through the transition-state theory and van't-Hoff-Arrhenius equation as follows [48]:

$$\tau = \upsilon_0^{-1} \exp\left(\frac{-E_{ads}}{k_B T}\right) \quad (4)$$

The ν_0, k_B, signifies the attempt frequency and Boltzmann's constant, respectively, at 298 K in UV irradiation ($\nu_0 \sim 800$ THz). This value of attempt frequency has been used for the calculation recovery time of the other nanosensors [49]. The calculated recovery time for desorption of the MDMA molecule in S_N, X_N, Y_N, M_N, and N_N complexes are 4.14×10^{16}, 1.8×10^4, 1.51, 4.45×10^{28}, and 5.02×10^{21} s, respectively. Thus, the computed recovery times are very long for the studied complexes except for adsorbed MDMA on the Si-$B_{12}N_{11}$ nanocage, showing its potential for utilizing in practical applications.

Humidity Effect on the Sensitivity of the Pristine, Si, and Al-doped $B_{12}N_{12}$ Nanocage

In continuation of the present research, humidity's influence as an essential parameter for designing the sensors is investigated. After optimizing the possible orientation for the disposition of one H_2O molecule over $B_{12}N_{12}$ nanocage, one stable complex is located, as displayed in Fig. 4. Furthermore, DOS for complexes of pristine, Si, and Al-doped $B_{12}N_{12}$ nanocage with water molecule plotted in Fig. 4. Finally, the calculated adsorption energy of H_2O and pristine, Si, and Al-doped $B_{12}N_{12}$ nanocage is tabulated in Table 3.

The results show that the adsorption energy of H_2O on Al-$B_{11}N_{12}$ nanocage is more potent than other investigated systems. The $\%\Delta E_g$ for pristine, Si, and Al-doped $B_{12}N_{12}$ nanocage after adsorption of H_2O are less than the corresponding values in complexes of MDMA drugs with studied frameworks. Albeit both water and MDMA molecules could be adsorbed onto pristine, Si, and Al-doped $B_{12}N_{12}$ nanocage, a substantial electric response is observed for MDMA molecules. The desired studied frameworks may detect MDMA drugs in the presence of dampness, assuming we exclude more significant amounts of water and the possible hydration of MDMA itself.

Drug Release from the Desired Si-$B_{12}N_{11}$ Nanocage

Recovery is a severe problem in biosensors, and this is related to the interaction mechanism between biomolecules and sensors' surfaces. Notably, one of the essential concerns in the biosensors is to recover the sensors in run-time and without accumulation of biomolecules on the sensor's surface. Diverse methods have been suggested in the literature to release the adsorbed molecules, such as the effect of oriented external electric field or recovery of sensors in the acidic environment. It was revealed that the applied electric field reduced the electron transfer between the biomolecules and the sensors [50-52]. Furthermore, H^+ species tend to link to the nucleophilic head of the biomolecules [53-55]. Accordingly, the interaction distances (interaction energies) between the molecules and the sensor in the acidic environment increase (decrease) compared to the nonacidic condition. Hence, the biomolecule and sensor interaction becomes weak; thus, the molecule can be released from the biosensor. The supposed drug-releasing procedure by applying an external electric field (EEF) is investigated and presented in continuing this research. While EEF of 0.001 and 0.005 a.u. in the direction of Si-N interaction for the desired MDMA--Si-$B_{12}N_{11}$ nanocage, E_{ads}, and Si--N intermolecular distance changed from -0.89 eV and 2.30 Å in the absence of EEF to -0.82, and -0.57 eV, and 2.33, and 2.43 Å, respectively. The weakening of E_{ads} and the elongation of the Si--N bond length due to the application of an external field make this method an effective strategy to release the studied MDMA drug from the desired sensor of the present study.

CONCLUSIONS

DFT calculations were utilized to study complexes of the pristine, Si, and Al-doped $B_{12}N_{12}$ nanocage with MDMA drugs. The considered drug is adsorbed outwardly of studied frameworks via the association between nitrogen atoms of the drug with appropriate atoms of the studied nanocage with maximum adsorption energy -2.57 eV. The band gap of all the studied nanocages is changed significantly with a maximum of 70% on account of the interaction of desired nanocages with the picked MDMA drug. Considering two factors, namely significant changes in electronic properties and appropriate recovery time, Si-$B_{12}N_{11}$ nanocage can be predominant adsorbent and felicitous recognizing vehicles for MDMA drug in certified operation even in the presence of water molecules. We hope that the present research results can be effective in practice in the fabrication of high-performance sensors for the detection of ecstasy drugs based on $B_{12}N_{12}$ nanocage.

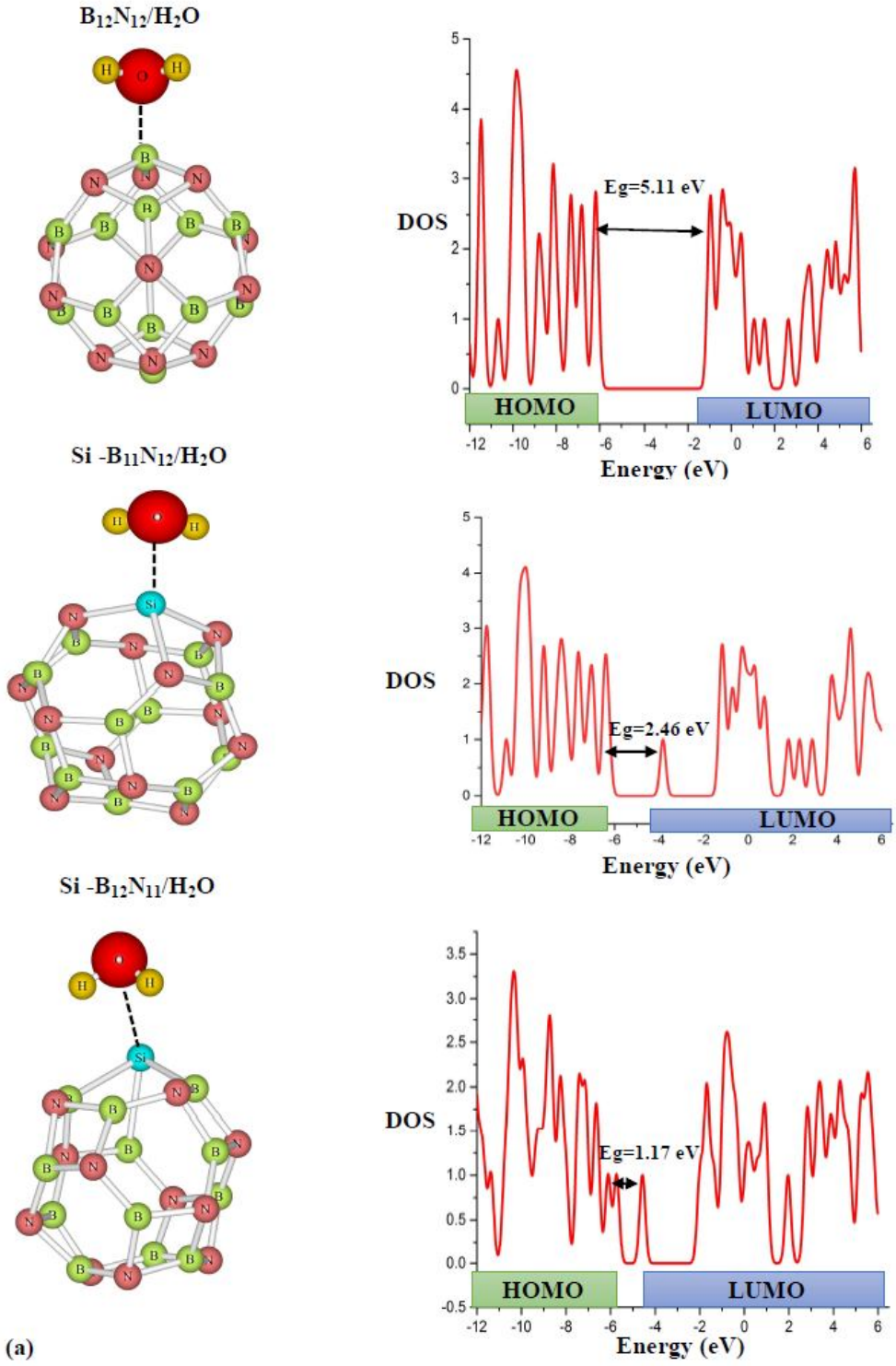

Fig. 4. Optimized structures, and density of states (DOS) of pristine, Si, and Al-doped $B_{12}N_{12}$ nanocage complexes with H_2O.

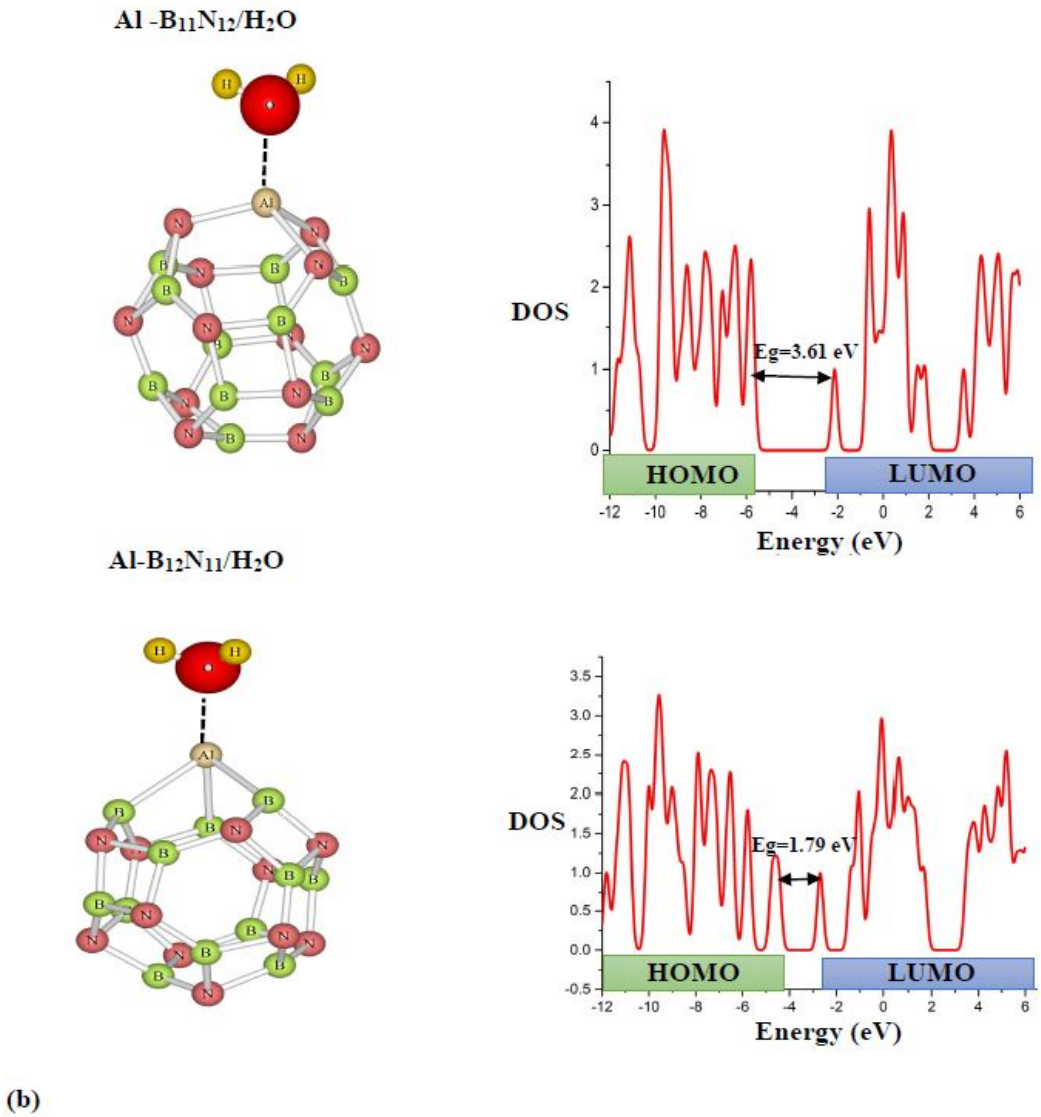

Fig. 4. Continued.

Table 3. The Calculated Adsorption Energy (E_{ads}) in eV, HOMO, LUMO Energies, HOMO-LUMO Energy Gap (Eg) in eV, and the Change of Energy Gap of Nanocage after Adsorption (%ΔE_g) of H_2O and Pristine, Si, and Al-doped $B_{12}N_{12}$ Nanocage

Systems	E_{ads} (eV)	HOMO (eV)	LUMO (eV)	Eg (eV)	ΔEg (%)
$B_{12}N_{12}/H_2O$	-0.77	-6.11	-1.00	5.11	-1.72
Si-$B_{11}N_{12}/H_2O$	-0.58	-6.28	-3.82	2.46	15.45
Si-$B_{12}N_{11}/H_2O$	-0.43	-5.73	-4.56	1.17	4.88
Al-$B_{11}N_{12}/H_2O$	-1.73	-5.73	-2.12	3.61	29.96
Al-$B_{12}N_{11}/H_2O$	-1.36	-4.47	-2.68	1.79	40.66

REFERENCES

[1] Yonzon, C. R.; Stuart, D. A.; Zhang, X.; McFarland, A. D.; Haynes, C. L.; Van Duyne, R. P., Towards advanced chemical and biological nanosensors -an overview. *Talanta*, **2005**, *67*, 438-448. DOI: 10.1016/j.talanta.2005.06.039.

[2] Chopra, N. G.; Luyken, R. J.; Cherrey, K.; Crespi, V. H.; Cohen, M. L.; Louie, S. G.; Zettl, A., Boron nitride nanotubes. *Science*, **1995**, *269*, 966. DOI: 10.1126/science.269.5226.966.

[3] Oku, T.; Hiraga, K.; Matsuda, T.; Hirai, T.; Hirabayashi, M., Formation and structures of multiply-twinned nanoparticles with fivefold symmetry in chemical vapor deposited boron nitride. *Diamond Relat. Mater.*, **2003**, *12*, 1918-1926. DOI: 10.1016/S0925-9635(03)00188-2.

[4] Iijima, S.; Brabec, C.; Maiti, A.; Bernholc, J., Structural flexibility of carbon nanotubes. *J. Chem. Phys.,* **1996**, *104*, 2089-2092. DOI: 10.1063/1.470966.

[5] Seifert, G.; Fowler, R. W.; Mitchell, D.; Porezag, D.; Frauenheim, Th., Boron-nitrogen analogues of the fullerenes: Electronic and structural properties., *Chem. Phys. Lett.,* **1997**, *268*, 352-358. DOI: 10.1016/S0009-2614(97)00214-5.

[6] Oku, T.; Nishiwaki, A.; Narita, I., Formation and atomic structure of $B_{12}N_{12}$ nanocage clusters studied by mass spectrometry and cluster calculation. *Sci. Technol. Adv. Mater.,* **2004**, *5*, 635. DOI: 10.1016/j.stam.2004.03.017/meta.

[7] Kim, J. H.; Pham, T. V.; Hwang, J. H.; Kim, C. S.; Kim, M. J., Boron nitride nanotubes: Synthesis and applications. *Nano Convergence*, **2018**, *5*, 1-13. DOI: 10.1186/s40580-018-0149-y.

[8] Yu, S.; Wang, X.; Pang, H.; Zhang, R.; Song, W.; Fu, D.; Hayat, T.; Wang, X., Boron nitride-based materials for the removal of pollutants from aqueous solutions: A review. *Chem. Eng. J.,* **2018**, *333*, 343-360. DOI: 10.1016/j.cej.2017.09.163.

[9] Yogi, R.; Jaiswal, N. K., Adsorption of CO gas molecules on zigzag BN/AlN nanoribbons for nano sensor applications. *Phys. Lett. A.,* **2019**, *383*, 532-538. DOI: 10.1016/j.physleta.2018.11.024.

[10] Mirkamali, E . S.; Ahmadi, R., Adsorption of melphalan anticancer drug on the surface of boron nitride cage ($B_{12}N_{12}$): A comprehensive DFT study. *J. Med. Chem. Sci*., **2020**, *3*, 199-207. DOI: 10.26655/ JMCHEMSCI.2020.3.1.

[11] Kalateh, K.; Abdolmanafi, A., Study of $B_{12}N_{12}$ and $AlB_{11}N_{12}$ Fullerene as H_2S Absorbent and sensor by computational method. *Int. J. New. Chem*., **2015**, *2*, 1-7. DOI: 10.22034/ IJNC.2015.15629.

[12] Vessally, E.; Ahmadi, E.; Esrafili, M. D.; Hosseinian, A., Adsorption and decomposition of formaldehyde on the $B_{12}N_{12}$ nanostructure: A density functional theory study. *Monatsh Chem,,* **2017**, *148*, 1727-1731. DOI: 10.1007/s00706-017-2003-z.

[13] Rad, A. S., Application of $B_{12}N_{12}$ and $B_{12}P_{12}$ as two fullerene-like semiconductors for adsorption of halomethane: Density functional theory study. *Semiconductors,* **2017**, *51*, 134-138. DOI: 10.1134/S1063782617010225.

[14] Peyghan, A. A.; Soleymanabadi, H., Computational study on ammonia adsorption on the $X_{12}Y_{12}$ nano-clusters (X = B, Al and Y = N, P). *Current Science,* **2015**, 1910-1914. DOI: jstor.org/stable/24905619.

[15] Beheshtian, J.; Bagheri, Z.; Kamfiroozi, M.; Ahmadi, A., Toxic CO detection by $B_{12}N_{12}$ nanocluster. *Microelectron. J.*, **2011**, 42, 1400-1403. DOI: 10.1016/j.mejo.2011.10.010.

[16] Quinonero, D.; Frontera, A.;. Deya, P. M, Feasibility of single-walled carbon nanotubes as materials for CO_2 adsorption: A DFT study. *J. Phys. Chem. C.,* **2012**, *116*, 21083-21092. DOI: 10.1021/jp306586f.

[17] Baei, M. T., Si-doped $B_{12}N_{12}$ nanocage as an adsorbent for dissociation of N_2O to N_2 molecule. *Heteroatom Chem.,* **2013**, *24*, 476-481. DOI: 10.1002/hc.21114.

[18] Beheshtian, J.; Peyghan, A. A.; Bagheri, Z.; Kamfiroozi, M., Interaction of small molecules (NO, H_2, N_2, and CH_4) with BN nanocluster surface. *Structural Chemistry.,* **2012**, *23*, 1567-1572. DOI: 10.1007/s11224-012-9970-9.

[19] Hussain, S.; Hussain, R.; Mehboob, M.Y.; Chatha, S.A.S.; Hussain, A.I.; Umar, A.; Khan, M.U.; Ahmed, M.; Adnan, M.; Ayub, K., Adsorption of Phosgene Gas on Pristine and Copper-Decorated $B_{12}N_{12}$ Nanocages: A Comparative DFT Study.

ACS Omega, **2020**, *5*, 7641-7650. DOI: 10.1021/acsomega.0c00507.

[20] Rostamoghli, R.; Vakili, M.; Banaei, A.; Pourbashir, E.; Jalalierad, K., Applying the $B_{12}N_{12}$ nanoparticle as the CO, CO_2, H_2O and NH_3 sensor. *Chem. Rev. Lett*., **2018**, *1*, 31-36. DOI: 10.22034/crl.2018.85214.

[21] Farrokhpour, H.; Jouypazadeh, H.; Vakili Sohroforouzani, S., Interaction of different types of nanocages ($Al_{12}N_{12}$, $Al_{12}P_{12}$, $B_{12}N_{12}$, $Be_{12}O_{12}$, $Mg_{12}O_{12}$, $Si_{12}C_{12}$ and C_{24}) with HCN and ClCN: DFT, TD-DFT, QTAIM, and NBO calculations. *Mol. Phys.* **2020**, *118*, 1626506. DOI: 10.1080/00268976.2019.1626506.

[22] Larki, S.; Shakerzadeh, E.; Anota, E. C.; Behjatmanesh-Ardakani, R., The Al, Ga and Sc dopants effect on the adsorption performance of $B_{12}N_{12}$ nanocluster toward pnictogen hydrides. *Chem. Phys.,* **2019**, *526*, 110424. DOI: 10.1016/j.chemphys.2019.110424.

[23] Jalali Sarvestani, M.; Ahmadi, R., Adsorption of tetryl on the surface of $B_{12}N_{12}$: A comprehensive DFT study. *Chem. Methodol.,* **2020**, *4*, 40-54. DOI: 10.33945/SAMI/CHEMM.2020.1.

[24] Fallahi, P.; Jouypazadeh, H.; Farrokhpour, H., Theoretical studies on the potentials of some nanocages ($Al_{12}N_{12}$, $Al_{12}P_{12}$, $B_{12}N_{12}$, $Be_{12}O_{12}$, $C_{12}Si_{12}$, $Mg_{12}O_{12}$ and C_{24}) on the detection and adsorption of Tabun molecule: DFT and TD-DFT study. *J. Mol. Liq.,* **2018**, *260*, 138-148. DOI: 10.1016/j.molliq.2018.03.085.

Shakerzadeh, E., A DFT study on the formaldehyde (H_2CO and $(H_2CO)_2$) monitoring using pristine $B_{12}N_{12}$ nanocluster. *Physica E*, **2016**, *78*, 19. DOI: 10.1016/j.physe.2015.11.038.

[25] Rad, A. S.; Ayub, K., O_3 and SO_2 sensing concept on extended surface of $B_{12}N_{12}$ nanocages modified by Nickel decoration: A comprehensive DFT study. *Solid State Sci*., **2017**, *69*, 22-30. DOI: 10.1016/j.solidstatesciences.2017.05.007.

[26] Rad, A. S.; Ayub, K., Adsorption of pyrrole on $Al_{12}N_{12}$, $Al_{12}P_{12}$, $B_{12}N_{12}$, and $B_{12}P_{12}$ fullerene-like nano-cages; a first principles study. *Vacuum*, **2016**, *131*, 135-141. DOI: 10.1016/j.vacuum.2016.06.012.

[27] Kaviani, S.; Shahab, S.; Sheikhi, M., Adsorption of alprazolam drug on the $B_{12}N_{12}$ and $Al_{12}N_{12}$ nano-cages for biological applications: A DFT study. *Physica E,* **2020**, *126*, 114473. DOI: 10.1016/j.physe.2020.114473.

[28] Abdolahi, N.; Aghaei, M.; Soltani, A.; Azmoodeh, Z.; Balakheyli, H.; Heidari, F., Adsorption of Celecoxib on $B_{12}N_{12}$ fullerene: Spectroscopic and DFT/TD-DFT study. *Spectrochim. Acta A,* **2018**, *204*, 348-353. DOI: 10.1016/j.saa.2018.06.077.

[29] Bahrami, A.; Seidi, Sh.; Baheri, T.; Aghamohammadi, M., A first-principles study on the adsorption behavior of amphetamine on pristine, P- and Al-doped $B_{12}N_{12}$ nano-cages. *Superlattices Microstruct.*, **2013**, *64*, 265-273. DOI: 10.1016/j.spmi.2013.09.034.

[30] Abdolahi, N.; Singla, P.; Soltani, A.; Javan, M.; Aghaei, M.; Heidari, F.; Sedighi, S., Gold decorated $B_{12}N_{12}$ nanocluster as an effective sulfasalazine drug carrier: A theoretical investigation. *Physica E,* **2020**, *124*, 114296. DOI: 10.1016/j.physe.2020.114296.

[31] Abbasi, M.; Nemati-Kande, E.; Mohammadi, M. D., Doping of the first row transition metals onto $B_{12}N_{12}$ nanocage: A DFT study. *Comput. Theor. Chem.,* **2018**, *1132*, 1-11. DOI: 10.1016/j.comptc.2018.04.003.

Baei, M. T., $B_{12}N_{12}$ sodalite like cage as potential sensor for hydrogen cyanide. *Comput. Theor. Chem.,* **2013**, *1024*, 28-33. DOI: 10.1016/j.comptc.2013.09.018.

[32] Rezaei-Sameti, M.; Jafari, M., Effect of Ni and Pd transition metal functionalized on interaction of mercaptopyridine with $B_{12}N_{12}$ nanocage: NBO, AIM, DFT, TD-DFT Study. *Chem. Methodol*., **2020**, *4*, 494-513. DOI: 10.33945/SAMI/CHEMM.2020.4.10.

[33] Majedi, S.; Rauf, H. G.; Boustanbakhsh, M., DFT study on sensing possibility of the pristine and Al-and Ga-embeded $B_{12}N_{12}$ nanostructures toward hydrazine and hydrogen peroxide and their analogues. *Chem. Rev. Lett*., **2019**, *2*, 176-186. DOI: 10.22034/CRL.2020.216625.1032.

[34] Ahmadi, R.; Jalali Sarvestani, M. R., Adsorption of proline amino acid on the surface of fullerene (C_20) and boron nitride cage ($B_{12}N_{12}$): A comprehensive DFT study. *Iran. Chem. Commun*., **2019**, *7*, 344-351. DOI: 10.30473/ICC.2018.40404.1437.

[35] Jouypazadeh, H.; Farrokhpour, H., DFT and TD-DFT study of the adsorption and detection of sulfur mustard chemical warfare agent by the C_{24}, $C_{12}Si_{12}$, $Al_{12}N_{12}$, $Al_{12}P_{12}$, $Be_{12}O_{12}$, $B_{12}N_{12}$ and $Mg_{12}O_{12}$ nanocages. *J. Mol. Struct*., **2018**, *1164*, 227-238. DOI: 10.1016/j.molstruc.2018.03.051.

[36] Jalali Sarvestani, M. R.; Ahmadi, R., Trinitroanisole adsorption on the surface of boron nitride nanocluster ($B_{12}N_{12}$): A computational study. *J. Water Environ. Nanotechnol.*, **2020**, *5*, 34-44. DOI: 10.22090/ JWENT.2020.01.003.

[37] Rad, A. S.; Ayub, K., Enhancement in hydrogen molecule adsorption on $B_{12}N_{12}$ nano-cluster by decoration of nickel. *Int. J. Hydrog. Energy*, **2016**, *41*, 22182-22191. DOI: 10.1016/j.ijhydene.2016.08.158.

[38] Solimannejad, M.; Kamalinahad, S.; Shakerzadeh, E., Sensing performance of Sc-doped $B_{12}N_{12}$ nanocage for detecting toxic cyanogen gas: A computational study. *Phys. Chem. Res.,* **2016**, *4*, 315-332. DOI: 10.22036/pcr.2016.14142.

[39] Zanfrognini, B.; Pigani, L.; Zanardi, C., Recent advances in the direct electrochemical detection of drugs of abuse. *J. Solid State Electrochem.*, **2020**, *24*, 2603-2616. DOI: 10.1007/s10008-020-04686-z.

[40] Reed, A. E.; Curtiss, L. A.; Weinhold, F., Intermolecular interactions from a natural bond orbital, donor-acceptor viewpoint. *Chem. Rev.,* **1988**, *88*, 899-926. DOI: 10.1021/cr00088a005.

[41] Fukui, K., The role of frontier orbitals in chemical reactions (Nobel Lecture). *Angew. Chem*., **1982**, *21*, 801-809. DOI: 10.1002/anie.198208013.

[42] Frisch, M.; Trucks, G.; Schlegel, H.; Scuseria, G.; Robb, M.; Cheeseman, J.; Montgomery Jr, J.; Vreven, T.; Kudin, K.; Burant, J., Pittsburgh P. A.; Pople, J. A., 2009, Gaussian 09, Revision A02. Gaussian Inc., Wallingford.

[43] Boys, S. F.; Bernardi, F., The Calculation of small molecular interactions by the differences of separate total energies. Some procedures with reduced errors. *Mol. Phys*., **1970**, *19*, 553-566. DOI: 10.1080/00268977000101561.

[44] O'boyle, N. M.; Tenderholt, A. L.; Langner, K. M., cclib: A library for package-independent computational chemistry algorithms. *J. Comput. Chem*., **2008**, *29*, 839-845. DOI: 10.1002/jcc.20823.

[45] Lu, T.; Chen, F., Multiwfn: A multifunctional wavefunction analyzer. *J. Comput. Chem.*, **2012**, *33*, 580-592. DOI: 10.1002/jcc.22885.

[46] Zhang, Y. H.; Chen, Y. B.; Zhou, K.Ge.; Hong Liu, C.; Zeng, J.; Zhang, H.Li.; Peng, Y., Improving gas sensing properties of graphene by introducing dopants and defects: a first-principles study. *Nanotechnology,* **2009**, *20*, 185504-185512. DOI: 10.1088/0957 4484/20/18/185504.

[47] Aghaei, S. M.; Monshi, M. M.; Torres, I.; Zeidi, S. M.; Calizo, I.; DFT study of adsorption behavior of NO, CO, NO_2, and NH_3 molecules on graphene-like BC_3: A search for highly sensitive molecular sensor. *Appl. Surf. Sci.,* **2018**, *427*, 326-333. DOI: doi.org/10.1016/j.apsusc.2017.08.048.

[48] Tokatli, A.; Tunç, F.; Ucun, F., Effect of external electric field on C-X ⋯ π halogen bonds. *J. Mol. Model.*, **2019**, *3*, 57. DOI: 10.1007/s00894-019-3938-2.

[49] Sarmah, N.; Bhattacharyya, P. K., Behaviour of cation-pi interaction in presence of external electric field. *RSC Adv.,* **2016**, *6*, 100008-100015. DOI: 10.1039/C6RA21334K.

[50] Deka, B. C.; Bhattacharyya, P. K., Reactivity of chitosan derivatives and their interaction with guanine: A computational study. *J. Chem. Sci.,* **2016**, *128*, 589-598. DOI: 10.1007/s12039-016-1064-6.

[51] Rahimi, R.; Solimannejad, M., First-principles survey on the pristine BC_2N monolayer as a promising vehicle for delivery of β-lapachone anticancer drug. *J. Mol. Liq.,* **2021**, *321*, 114917. DOI: 10.1016/j.molliq.2020.114917.

[52] Rahimi, R.; Solimannejad, M.; BC_3 graphene-like monolayer as a drug delivery system for nitrosourea anticancer drug: A first-principles perception. *Appl. Surf. Sci*., **2020**, *525*, 146577. DOI: 10.1016/j.apsusc.2020.146577.

[53] Hazrati, M. K.; Javanshir, Z.; Bagheri, Z., $B_{24}N_{24}$ fullerene as a carrier for 5-fluorouracil anti-cancer drug delivery: DFT studies. *J. Mol. Graph. Model.,* **2017**, *77*, 17-24. DOI: 10.1016/j.jmgm.2017.08.003.